Journal of
Materials Chemistry C

PAPER

View Article Online
View Journal | View Issue

Cite this: *J. Mater. Chem. C*, 2018, **6**, 7576

Design of novel graphdiyne-based materials with large second-order nonlinear optical properties†

Xiaojun Li

Received 3rd May 2018,
Accepted 20th June 2018

DOI: 10.1039/c8tc02146e

rsc.li/materials-c

In this study, we designed a series of new alkali metal-adsorbed graphdiyne (GDY) structures (denoted as AM_3@GDY (AM = Li, Na, K)) with an intramolecular electron donor–acceptor framework using density functional theory calculations. It is found that the three alkali metals are energetically preferred to be adsorbed on the three hollows of the largely delocalized π-conjugated GDY surface, while the adsorption of alkali metals largely affects the electronic properties of the complexes, and reduces the vertical ionization potentials. More interestingly, the doping of alkali metal atoms dramatically enhances the static first hyperpolarizabilities (β_{tot}) of AM_3@GDY, of which the K_3@GDY cluster possesses a remarkably giant β_{tot} value of $\sim 1.61 \times 10^5$ a.u., which is enough for it to exhibit strong nonlinear optical (NLO) behavior. These findings may provide new insights into the design of novel graphdiyne-based NLO materials and promote further potential applications in optoelectronic nanodevices.

1 Introduction

It is well-known that carbon materials have attracted a lot of attention because of their potential applications in microelectronic fields, *e.g.*, optoelectronics,[1,2] catalysis,[3–5] sensors,[6–8] energy storage,[9–12] and environmental pollution,[13,14] and so on. Especially, the two dimensional (2D) carbon materials with a largely delocalized π-conjugated architecture have been widely focused upon due to their promising physical and chemical properties, and can be considered as possible candidates of the next-generation optoelectronic nanodevices,[15–17] after an atomically single-layer graphene film was successfully prepared in 2004.[18] Recently, there have also been many previous theoretical and experimental studies on the nonlinear optical (NLO) materials since the common NLO crystals (*e.g.*, β-BaB_2O_4,[19] LiB_3O_5,[20] *et al.*) were commercially synthesized and applied as high-performance optoelectronic devices. For example, Meyer *et al.*[21] synthesized a new compound $Ca_3(O_3C_3N_3)_2$, and a higher second harmonic generation (SHG) efficiency was found for the crystal. Moreover, it is also known that the barium borate crystal, composed of planar delocalized π-conjugated $(B_3O_6)^{3-}$ anions,[22,23] possesses excellent NLO properties, as well as for planar $(C_3N_3O_3)^{3-}$ anions,[24] while the SHG response can be remarkably enhanced by a localized π-orbital O_2 group.[25] More interestingly, some alkali-metal fluorooxoborates, AB_4O_6F (F = K, Rb, Cs), are also reported to exhibit large SHG responses.[26] Accordingly, the molecular structures containing a largely π-conjugated network may be designed as the fundamental building blocks for exploring novel promising NLO materials,[27–29] especially for the 2D structures, and the π-conjugation length and electron donor–acceptor process of these species could largely enhance the nonlinear optical properties, *e.g.*, hybridized graphene nanoribbons made by intercalating hexagonal boron nitride can generate a strong third-order NLO response.[30] To date, it is still challenging for researchers to synthesize novel 2D carbon materials with a largely π-conjugated network for basic studies and extending their various applications.

Fortunately, a new carbon allotrope (graphdiyne, GDY, Fig. 1(a)) with sp- and sp^2-hybridized carbon atoms through incorporation of diacetylenic linkages has been successfully synthesized experimentally using the cross-coupling mechanism with hexaethynyl benzene on the surface of copper.[31] The structure has an ordered regular arrangement of self-assembled 18-member ring (18MR) hexagonal units with three large hollows in planar layers, forming a largely delocalized π-conjugated framework, which may produce fascinating electronic and optical properties, which are very different from those of the graphene layer, *e.g.*, large nonlinear optical susceptibility,[32] high electronic conductivity and mobility,[33–35] extreme thermal resistance,[36] *etc.* Moreover, it is expected that the graphdiyne materials can be experimentally and theoretically applied in hydrogen storage[37,38] and purification,[39] electrode materials,[40,41] catalysis,[42–44] and optoelectronic devices,[45,46] *etc.* Most intriguingly, the doping of metal atoms into GDY has attracted great interest, as it can effectively tailor the electronic properties of GDY. For example, a single metal-adsorbed GDY sheet was studied using density functional theory (DFT)

The Key Laboratory for Surface Engineering and Remanufacturing in Shaanxi Province, School of Chemical Engineering, Xi'an University, Xi'an 710065, Shaanxi, P. R. China. E-mail: xjli@xawl.edu.cn

† Electronic supplementary information (ESI) available: Simulated infrared spectrum of the GDY cluster, Fig. S1; electrostatic potential maps of the GDY and AM_3@GDY clusters, Fig. S2; and the crucial transitions of crucial excited energies for the AM_3@GDY clusters, Table S1. See DOI: 10.1039/c8tc02146e

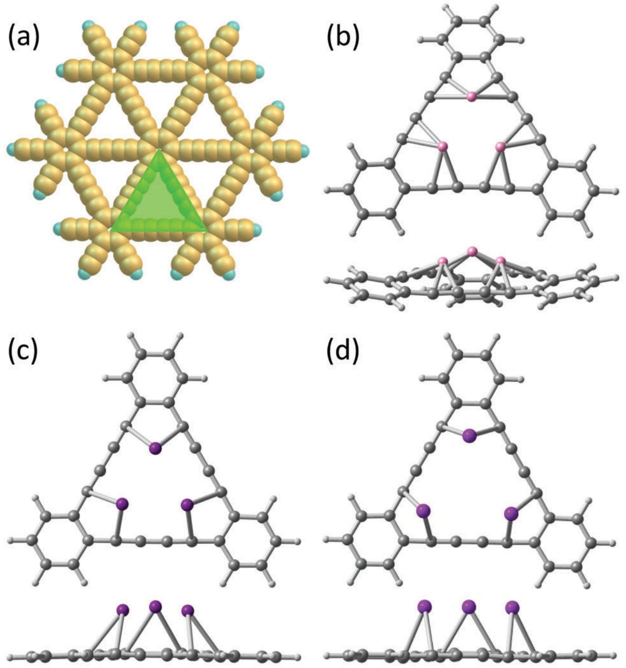

Fig. 1 Schematic structure of (a) single-layer graphdiyne (GDY), in which the shaded region represents the 18-member ring hexagon unit, and optimized stable structures of (b) Li_3@GDY, (c) Na_3@GDY, and (d) K_3@GDY clusters. The gray, white, and colorized balls represent the C, H, and alkali metals, respectively.

calculations,[47] and it is found that the adsorption of metal atoms not only changes the electronic structures of GDY, but also produces excellent magnetic behaviors. Very recently, Li and co-worker[48] also reviewed several new methods for the synthesis of graphdiyne, and designed a graphdiyne-supported transition-metal catalyst for hydrogen evolution[49,50] and lithium/sodium ion batteries with high conductivity and capacity.[51–53] Actually, it is known that the three alkali metal atoms (Li, Na, K) can structurally interact with the three hollows on the delocalized GDY surface, forming the intramolecular electron donor–acceptor (D–π–A) process due to the small ionization potentials of these alkali metals,[54] which provides the possible conditions for enhancing the NLO properties,[55,56] *e.g.*, the static first hyperpolarizability.

In this paper, we attempt to perform a series of calculations for exploring alkali metal-adsorbed graphdiyne (GDY) structures, denoted as AM_3@GDY (AM = Li, Na, K), while their electronic properties and nonlinear optical behaviors are systematically studied by using density functional theory calculations. More impressively, the adsorption of alkali metal atoms remarkably enhances the static first hyperpolarizabilities (β_{tot}) of the AM_3@GDY clusters, especially for K_3@GDY, which possesses a giant β_{tot} value of $\sim 1.61 \times 10^5$ a.u., and may be considered as a promising novel graphdiyne-based NLO material.

2 Computational details

All structural optimizations of the AM_3@GDY (AM = Li, Na, and K) systems are performed using the hybrid B3LYP functional,[57,58] with the 6-31+G(d) basis set as implemented in the Gaussian 09 program.[59] We have also considered the weak interaction correction, *e.g.*, dispersion DFT-D3,[60–62] which is properly applied for the prediction of the structural properties of systems. In order to test the calculation method, our simulated infrared spectrum of GDY (Fig. S1, ESI†) is compared with previous theory,[63] in which two major vibrational peaks for the C≡C stretching modes are calculated to be 2131 and 2205 cm^{-1}, being consistent with the previous predictions of 2135 and 2200 cm^{-1}, respectively, and thus the method is more reliable for the structural prediction of the systems. The natural charges were evaluated to explore the charge-transfer (CT) mechanism between the alkali metals and GDY cluster, by means of a natural population analysis (NPA) method using the NBO 6.0 program.[64] The linear and nonlinear optical properties of the systems, *e.g.*, polarizability (α) and first hyperpolarizability (β), were calculated by using a long-range corrected CAM-B3LYP functional[65] with the all-electron 6-311++G(2d,2p) basis sets, because the method has been confirmed to be very reliable for the evaluation of various species,[66–69] as well as for the evaluation of the crucial excited energies (ΔE) and oscillator strength (f) within the framework of time-dependent density functional theory (TDDFT)[70] at the TD-CAM-B3LYP/6-31+G(d) level of theory. Harmonic vibrational frequencies were employed to confirm that these structures studied here correspond to real local minima on the potential energy surface (PES). Partial density of states (PDOS) spectra were convoluted utilizing the GaussSum 2.2 program[71] with a full-width at half maximum (FWHM) of 0.3 eV. The molecular graphs were visualized using the VMD program.[72]

The energy of a system is a function of the homogeneous electric field, and its Taylor expansion with respect to the field can be expressed as the following equation:[73–75]

$$E(F) = E^0 - \mu_i F_i - \frac{1}{2}\alpha_{ij}F_iF_j - \frac{1}{6}\beta_{ijk}F_iF_jF_k - \frac{1}{24}\gamma_{ijkl}F_iF_jF_kF_l\cdots \quad (1)$$

where E^0 is the system energy in the absence of an electric field and F_i is the electric field component along the i direction. The μ_i, α_{ij}, and β_{ijk} terms are the dipole moment, polarizability, and first hyperpolarizability, respectively, of which β_{ijk} is recognized as a second-order nonlinear optical (NLO) response coefficient.[76] The mean dipole moment (μ_0), static polarizability (α_0), and static first hyperpolarizability (β_{tot}) are defined as follows:

$$\mu_0 = ({\mu_x}^2 + {\mu_y}^2 + {\mu_z}^2)^{1/2} \quad (2)$$

$$\alpha_0 = (\alpha_{xx} + \alpha_{yy} + \alpha_{zz})/3 \quad (3)$$

$$\beta_{tot} = ({\beta_x}^2 + {\beta_y}^2 + {\beta_z}^2)^{1/2} \quad (4)$$

where $\beta_i = (1/3)\sum_j \left(\beta_{ijj} + \beta_{jji} + \beta_{jij}\right) \quad i,j = \{x,y,z\}$.

3 Results and discussion

3.1 Structure and chemical stability

To search the equilibrium structures, we have considered different positions on the largely delocalized π-conjugated GDY surface to adsorb alkali metals, and the optimized structures of the AM_3@GDY (AM = Li, Na, and K) clusters are presented in Fig. 1(b–d), of which the three alkali metal atoms are located at the stable positions above three hollows on the GDY surface. Based on our calculations, it is mentioned that the Li_3-adsorbed GDY cluster has a distorted GDY surface whereas the other two clusters present a planar GDY framework. The average equilibrium AM–C bond distances of AM_3@GDY (AM = Li, Na, K) are obviously increased as the atomic number of alkali metals from Li to K increases: 2.246 (Li) Å < 2.935 (Na) Å < 2.954 (K) Å.

For exploring the binding stability of AM_3@GDY, the binding energies (E_b) are estimated using the following equation:

$$E_b = E(\text{GDY}) + 3 \times E(\text{AM}) - E(\text{AM}_3@\text{GDY}),\ \text{AM} = \text{Li, Na, K} \quad (5)$$

where E(GDY), E(AM), and E(AM_3@GDY) are the total energies of pure GDY, alkali metals, and complexes, respectively. The E_b values of the AM_3@GDY clusters are displayed in Fig. 2(a). It can be found that all E_b values of the considered systems are largely positive, indicating that these complexes are rather stable against dissociation into the AM_3 moieties. In particular, the Li_3@GDY cluster has the largest E_b value (4.52 eV) among these complexes, and this shows that the interactions between the Li atoms and the GDY cluster are much stronger. Meanwhile, the strong chemisorption features can be understood by the presence of a strong charge-transfer mechanism from the alkali metals to GDY, reflected by the electrostatic potential maps (Fig. S2, ESI†). To further explore the structural stability of these AM_3@GDY complexes, the charge density differences (CDD, $\Delta\rho$) were determined by using the B3LYP functional, and are plotted in Fig. 2. As shown in Fig. 2(b–d), a great number of electrons leave the Li_3 moiety, and the transferred electrons are largely accumulated on the GDY surface of Li_3@GDY. In contrast, a few electrons are transferred for the other two complexes, especially for Na_3@GDY, which is consistent with their relative stabilities reflected by the binding energies.

3.2 Electronic properties and charge transfer

To systematically study the electronic properties of the AM_3@GDY clusters, we plotted the total (TDOS) and partial (PDOS) density of states for all the considered systems, which includes the fragment contributions (AM_3 and GDY-C) in these clusters, as depicted in Fig. 2(b–d). As evidenced by the diagram, it can be seen that for all the clusters, the GDY-C fragment mainly contributes to the occupied orbitals of TDOS, whereas the alkali metals have a minor contribution to the occupied states. At the same time, one can clearly observe from Fig. 2 that the electronic features largely originate from alkali metals near the Fermi level, which are responsible for the structural stability of these studied clusters. More impressively, the HOMO–LUMO gaps for AM_3@GDY are predicted to be 0.81–1.19 eV, and the energy gaps

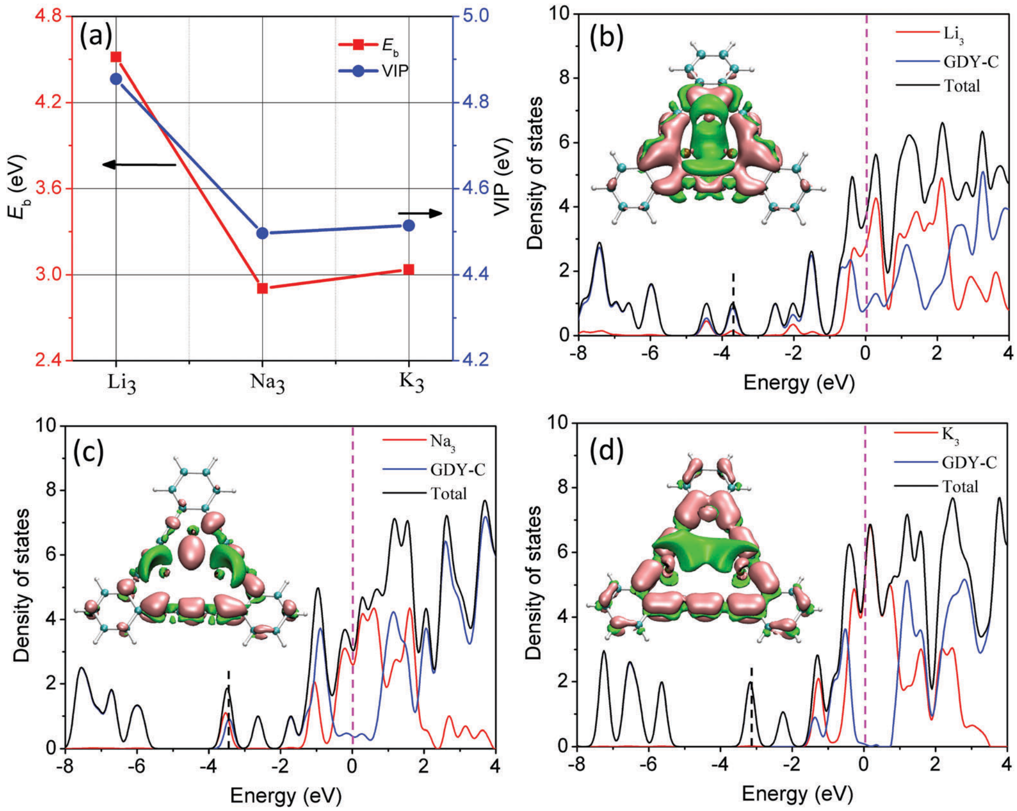

Fig. 2 (a) The binding energy (E_b) and vertical ionization potentials (VIP) of the AM_3@GDY (AM = Li, Na, and K) clusters, and the density of states (DOS) of (b) Li_3@GDY, (c) Na_3@GDY, and (d) K_3@GDY. The dashed lines correspond to the HOMO orbitals, and the Fermi level is shifted to zero. The charge density differences (CDDs, $\Delta\rho = \rho(AM_3@GDY) - \rho(GDY) - \rho(AM_3)$) are inserted, in which the pink and green regions represent the charge accumulation and depletion, respectively.

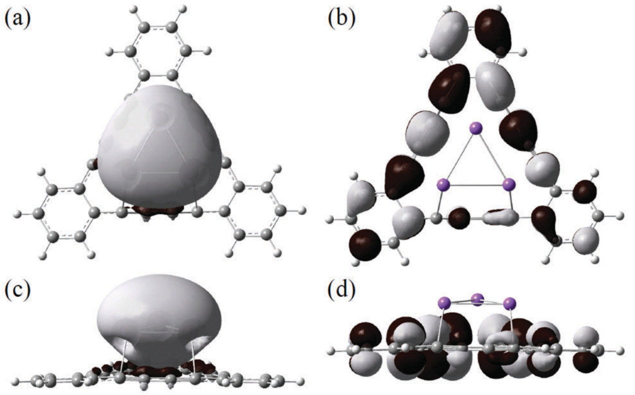

Fig. 3 HOMO (a and c) and LUMO (b and d) orbital plots of the Na_3@GDY cluster: (a and b) top view, (c and d) side view.

will be mostly associated with charge density redistributions of the HOMO and LUMO, *e.g.*, taking Na_3@GDY as an example (Fig. 3), in which the excess electrons accumulate on the Na_3 moieties of the HOMO.

The NPA charges on the AM_3 moieties in these AM_3@GDY (AM = Li, Na, K) clusters, obtained at the B3LYP/6-31+G* level of theory, are given in Table 1. Obviously, all NPA charges on the alkali metals have positive values in the range of 0.209–0.686$|e|$, of which the Na atoms occupy small charges (0.209–0.387$|e|$). Meanwhile, the total charges (Q_{tot}) on the AM_3 moieties are 0.946–1.963$|e|$, indicating that the electrons transfer obviously from the AM_3 moieties to the GDY fragment, leading to the intramolecular electron donor–acceptor (D–π–A) process. Noteworthily, the NBO results also show us the strong alkalide features of the systems, and may induce large nonlinear optical properties. The calculated vertical ionization potentials (VIPs) are listed in Table 1, and the AM_3@GDY (AM = Li, Na, K) clusters are predicted to have a smaller ionization potential (4.50–4.85 eV) than that (5.389 eV) of the Li atom,[54] and can be considered as novel superalkali compounds. As shown in Table 1, the VIP values of AM_3@GDY are mainly correlated with the alkali metal atoms, and present a decreasing tendency in the order: Li_3@GDY (4.85 eV) > Na_3@GDY (4.50 eV) ≈ K_3@GDY (4.51 eV).

Table 1 The calculated charges on alkali metal atoms (Q_{AM1}, Q_{AM2}, Q_{AM3}), and the total charges (Q_{tot}) on the AM_3 moieties, the predicted vertical ionization potentials (VIP, in eV), dipole moment (μ_0, in a.u.), polarizability (α_0, in a.u.), first hyperpolarizability (β_{tot}, in a.u.), maximum oscillator strength (f_0, in a.u.), change in dipole moments ($\Delta\mu$, in a.u.), and transition energies (ΔE, in eV) of crucial excited energies for the AM_3@GDY (AM = Li, Na, K) complexes

Properties	GDY[a]	Li_3@GDY	Na_3@GDY	K_3@GDY
Q_{AM1}	—	0.686	0.350	0.653
Q_{AM2}	—	0.639	0.209	0.641
Q_{AM3}	—	0.638	0.387	0.643
Q_{tot}	—	1.963	0.946	1.937
VIP	—	4.85	4.50	4.51
μ_0	0.00	0.84	1.62	3.32
α_0	459.08	671.19	786.44	1065.49
β_x	—	−121.14	66 020.46	−30 248.82
β_y	—	7861.59	−22 155.09	−47 726.76
β_z	—	−4794.19	−4566.14	−150 973.60
β_{tot}	0.13	9208.88	69 788.24	161 201.31
f_0	0.991	0.178	0.232	0.777 (0.315)
$\Delta\mu$	10.75	2.186	3.444	10.650 (6.735)
ΔE	3.76	3.32	2.75	2.98 (1.91)

[a] The values were taken from ref. 77 and are calculated at the CAM-B3LYP/6-31+G(d) level of theory.

3.3 Nonlinear optical properties

Here, the static polarizability (α_0) and the first hyperpolarizability (β_{tot}) of the AM_3@GDY (AM = Li, Na, K) clusters were studied at the CAM-B3LYP/6-311++G(2d,2p) level of theory, in order to explore their nonlinear optical behaviors, as shown in Table 1. Apparently, the polarizability of pure GDY is only 459.08 a.u., but the adsorption of the AM_3 alkali metals on the largely delocalized π-conjugated GDY surface can obviously increase the α_0 values of AM_3@GDY with the increasing atomic radii of the alkali atoms from Li to K: 671.19 a.u. < 786.44 a.u. < 1065.49 a.u. One can see from Table 1 that the static first hyperpolarizability (β_{tot}) of the pure GDY cluster is predicted to be 0.13 a.u. in the previous report,[77] indicating that the optical properties of this cluster are very tiny. After doping the AM_3 alkali metals, the β_{tot} values of the AM_3@GDY (AM = Li, Na, K) clusters are dramatically enhanced, being 9208.88, 69788.24, and 161 201.31 a.u., respectively, and can be determined by the alkalide features of alkali metal atoms, because the valence electrons of alkali metal atoms are easily transferred to the GDY framework once alkali metal atoms are interacted with GDY. Moreover, the β_{tot} values of the AM_3@GDY clusters are obviously larger than that (3977.40 a.u.) of the functionalized GDY cluster substituted by a Na atom on the hexagonal ring.[77] This result shows that the intramolecular charge-transfer occurring in the D–π–A process plays an important role in enhancing the NLO behaviors, rather than substitution on the hexagonal ring. Noteworthily, the first hyperpolarizabilities of the studied systems are quite enough to explore their NLO behaviors, because these clusters exhibit particularly significant β_{tot} values induced by the AM_3 alkali metals, *e.g.*, as high as 1.61×10^5 a.u. for K_3@GDY, which is comparable to those of Li_2@BN-clusters (8,0) ($\sim 1.23 \times 10^4$ a.u.),[78] Li_2F ($\sim 1.23 \times 10^4$ a.u.),[79] NO_2–HBC–NH_2 ($\sim 2.67 \times 10^4$ a.u.),[80] OLi_3–K–Li_3O ($\sim 1.94 \times 10^4$ a.u.),[81] and Na@Ge_7Au ($\sim 1.31 \times 10^4$ a.u.).[82] According to our results, it is hopeful that this work may not only predict a series of new superalkali compounds, but also provide an effective strategy to strengthen the nonlinear optical properties of the GDY-based carbon materials.

In order to efficiently explore the giant NLO properties, we have evaluated the crucial electronic transitions on these AM_3@GDY clusters by TDDFT calculations, as shown in Fig. 4. The static first hyperpolarizability from the two-level expression[73,83] can be defined as follows:

$$\beta_{\text{tot}} \propto \frac{\Delta\mu \cdot f_0}{\Delta E^3} \tag{6}$$

where β_{tot} is proportional to the largest oscillator strength (f_0) and the difference ($\Delta\mu$) of dipole moments between the ground state and the crucial excited state, but inversely proportional to the third

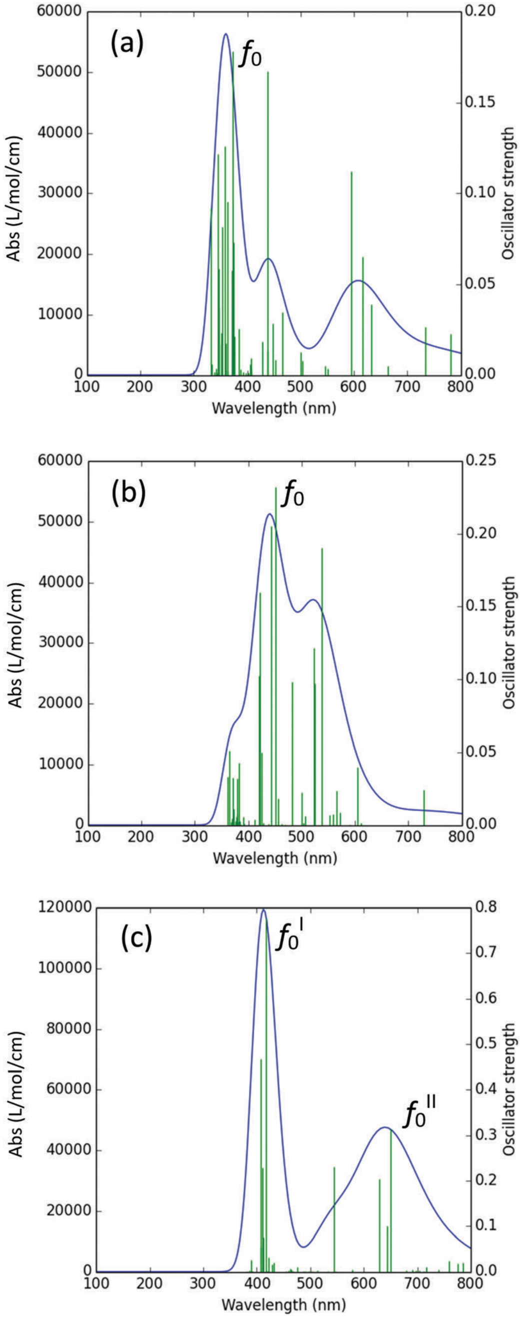

Fig. 4 Simulated optical absorption spectra of the (a) Li_3@GDY, (b) Na_3@GDY, and (c) K_3@GDY clusters using the CAM-B3LYP method. Their oscillator strengths are inserted.

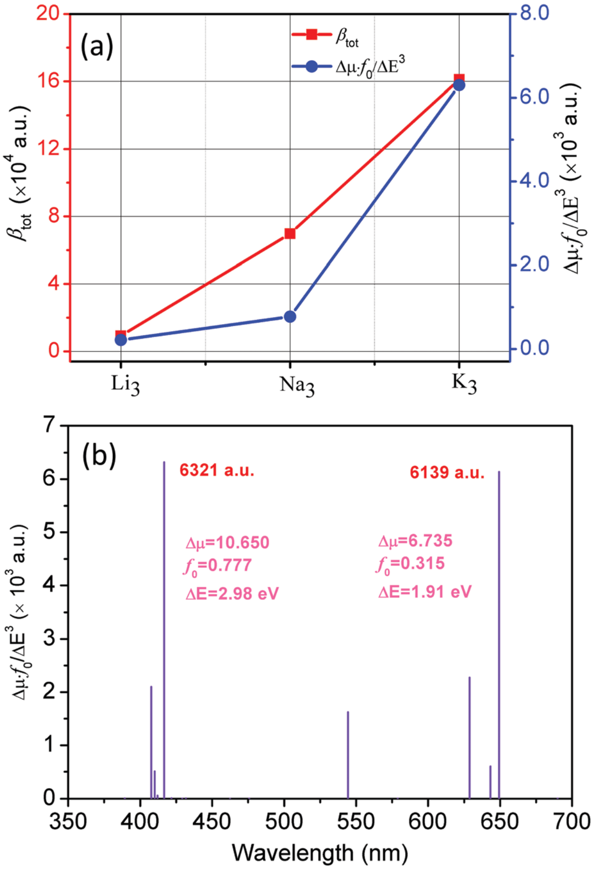

Fig. 5 Plots of (a) comparison of exactly calculated static first hyperpolarizability (β_{tot}) and estimated by two-level model ($\Delta\mu{\cdot}f_0/\Delta E^3$) for AM_3@GDY (AM = Li, Na, and K), and (b) the evaluated $\Delta\mu{\cdot}f_0/\Delta E^3$ values *versus* wavelengths of electronic transitions of the K_3@GDY cluster.

power of transition energy (ΔE) of the crucial excited states. The ΔE, f_0, and $\Delta\mu$ of the crucial excited states for the considered systems are listed in Table 1, and the crucial electronic transitions are shown in Table S1 (ESI†). To better visualize the dependences of the β_{tot} values approximately evaluated by the two-level model and exactly calculated by the DFT method on the alkali metals from Li to K, the variation trends are plotted in Fig. 5(a). It is noticeable that the β_{tot} values evaluated by the two-level expression and exactly calculated by DFT have a similar increased behavior. As for the Na_3@GDY cluster, however, the correlations of approximately evaluated and exactly calculated β_{tot} are slightly worse, due to the possible non-negligible contributions of excited states, and the crucial excited state still plays an important role in evaluating the β_{tot} value. The crucial states with the largest f_0 of these AM_3@GDY clusters can be found in simulated optical absorption spectra (Fig. 4). As discussed above, the two-level expression can be applied to explain the large NLO properties, here we also plotted the evaluated $\Delta\mu{\cdot}f_0/\Delta E^3$ values *versus* the wavelengths of electronic transitions of K_3@GDY in order to visualize the TDDFT results, and the two strong electronic absorption peaks with the transition energies (2.98 and 1.91 eV) make the dominant contributions to the β_{tot} value, rather than the other peaks, see Fig. 5(b), while the two main electronic transitions in crucial excited states for K3@GDY are displayed for understanding the contributions (Fig. 6). Thus, it is reasonable that the K_3@GDY cluster possesses the largest β_{tot} value ($\sim 1.61 \times 10^5$ a.u.), and the transition energies of the crucial excited states are also one of the decisive factors for predicting the large static first hyperpolarizability.

4 Conclusions

In summary, we have systematically investigated the structural, electronic and nonlinear optical properties of the AM_3@GDY

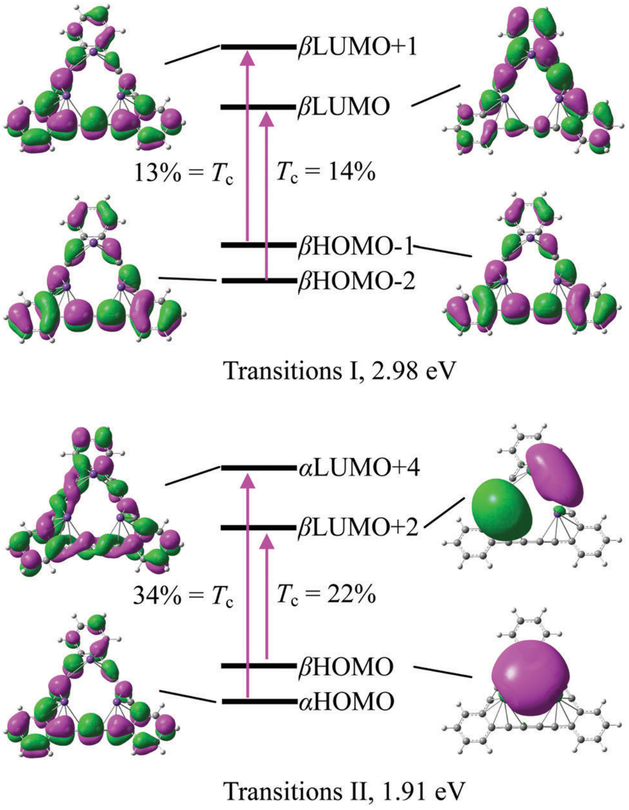

Fig. 6 Two main electronic transitions (I and II) in crucial excited states (T_c) for the K_3@GDY cluster, calculated using the CAM-B3LYP method.

(AM = Li, Na, K) clusters using density functional theory calculations. Our results show that the three alkali metal atoms are preferred for energy to be adsorbed on the three hollows of a largely delocalized π-conjugated GDY surface, and the Li_3@GDY cluster has the largest E_b value (4.52 eV) among these complexes. Obviously, the adsorptions of alkali metals affect the electronic properties of the GDY cluster and reduce the vertical ionization potentials, and they are considered as novel superalkali compounds, while the electrons transfer from alkali metal moieties to the GDY fragment to form the intramolecular D–π–A process. Interestingly, it is predicted that the AM_3@GDY clusters have large static first hyperpolarizabilities (β_{tot}), especially for K_3@GDY, which possesses remarkably giant β_{tot} values up to $\sim 1.61 \times 10^5$ a.u., and are quite enough to perform the enhanced NLO behaviors. Moreover, the two-level expression evaluated by TDDFT calculations can be used to further explain the large NLO properties. The present results will inevitably stimulate future experimental and theoretical studies of the largely π-conjugated GDY clusters by absorbing the alkali metals to design novel graphdiyne-based nanodevices and NLO materials.

Conflicts of interest

There are no conflicts to declare.

Acknowledgements

This work was supported by the National Natural Science Foundation of China (No. 21603173), the Natural Science Foundation of Shaanxi Province (No. 2016JQ5110), and the Natural Science Foundation of Science and Technology Bureau of Xi'an City (No. 2016CXWL16).

Notes and references

1 X. Li, L. Tao, Z. Chen, H. Fang, X. Li, X. Wang, J.-B. Xu and H. Zhu, *Appl. Phys. Rev.*, 2017, **4**, 021306.
2 S. A. Maksimenko and Y. Svirko, *J. Nanophotonics*, 2017, **11**, 032501.
3 D. Deng, K. S. Novoselov, Q. Fu, N. Zheng, Z. Tian and X. Bao, *Nat. Nanotechnol.*, 2016, **11**, 218–230.
4 W. Yang, X. Liu, X. Yue, J. Jia and S. Guo, *J. Am. Chem. Soc.*, 2015, **137**, 1436–1439.
5 S. Vidal, J. Marco-Martínez, S. Filippone and N. Martín, *Chem. Commun.*, 2017, **53**, 4842–4844.
6 S. Sotiropoulou, V. Gavalas, V. Vamvakaki and N. A. Chaniotakis, *Biosens. Bioelectron.*, 2003, **18**, 211–215.
7 Q. He, S. Wu, Z. Yin and H. Zhang, *Chem. Sci.*, 2012, **3**, 1764–1772.
8 J. P. Łukaszewicz, *Sens. Lett.*, 2006, **4**, 53–98.
9 X. Yang, C. Cheng, Y. Wang, L. Qiu and D. Li, *Science*, 2013, **341**, 534–537.
10 Y. Zhai, Y. Dou, D. Zhao, P. F. Fulvio, R. T. Mayes and S. Dai, *Adv. Mater.*, 2011, **23**, 4828–4850.
11 D.-W. Wang, F. Li, M. Liu, G. Q. Lu and H.-M. Cheng, *Angew. Chem., Int. Ed.*, 2007, **47**, 373–376.
12 J.-H. Guo, H. Zhang and Y. Miyamoto, *Phys. Chem. Chem. Phys.*, 2013, **15**, 8199–8207.
13 E. Lam and J. H. T. Luong, *ACS Catal.*, 2014, **4**, 3393–3410.
14 G. Mamba and A. K. Mishra, *Appl. Catal., B*, 2016, **198**, 347–377.
15 X. Li, M. Rui, J. Song, Z. Shen and H. Zeng, *Adv. Funct. Mater.*, 2015, **25**, 4929–4947.
16 J. Du, S. Pei, L. Ma and H. Cheng, *Adv. Mater.*, 2014, **26**, 1958–1991.
17 Y. Liu, F. Wang, X. Wang, X. Wang, E. Flahaut, X. Liu, Y. Li, X. Wang, Y. Xu, Y. Shi and R. Zhang, *Nat. Commun.*, 2015, **6**, 8589.
18 K. S. Novoselov, A. K. Geim, S. V. Morozov, D. Jiang, Y. Zhang, S. V. Dubonos, I. V. Grigorieva and A. A. Firsov, *Science*, 2004, **306**, 666–669.
19 D. Guiqin, L. Wei, Z. An, H. Qingzhen and L. Jingkui, *J. Am. Ceram. Soc.*, 1990, **73**, 2526–2527.
20 C. Chen, Y. Wu, A. Jiang, B. Wu, G. You, R. Li and S. Lin, *J. Opt. Soc. Am. B*, 1989, **6**, 616–621.
21 M. Kalmutzki, M. Ströbele, F. Wackenhut, A. J. Meixner and J. Meyer, *Angew. Chem., Int. Ed.*, 2014, **53**, 14260–14263.
22 J. Lin, M.-H. Lee, Z.-P. Liu, C. Chen and C. J. Pickard, *Phys. Rev. B: Condens. Matter Mater. Phys.*, 1999, **60**, 13380.
23 F. Liang, L. Kang, P. Gong, Z. Lin and Y. Wu, *Chem. Mater.*, 2017, **29**, 7098–7102.

24 F. Liang, L. Kang, X. Zhang, M.-H. Lee, Z. Lin and Y. Wu, *Cryst. Growth Des.*, 2017, **17**, 4015–4020.

25 Y. Song, M. Luo, F. Liang, N. Ye and Z. Lin, *Chem. Commun.*, 2018, **54**, 1445–1448.

26 Y. Wang, B. Zhang, Z. Yang and S. Pan, *Angew. Chem., Int. Ed.*, 2018, **57**, 2150–2154.

27 C. Hu, Z. Chen, H. Xiao, Z. Zhen, X. Liu and S. Bo, *J. Mater. Chem. C*, 2017, **5**, 5111–5118.

28 F. Liu, Y. Yang, S. Cong, H. Wang, M. Zhang, S. Bo, J. Liu, Z. Zhen, X. Liu and L. Qiu, *RSC Adv.*, 2014, **4**, 52991–52999.

29 H. Chakraborti, *Spectrochim. Acta, Part A*, 2016, **153**, 226–230.

30 M. Zhang, G. Li and L. Li, *J. Mater. Chem. C*, 2014, **2**, 1482–1488.

31 G. Li, Y. Li, H. Liu, Y. Guo, Y. Li and D. Zhu, *Chem. Commun.*, 2010, **46**, 3256–3258.

32 A. Bhaskar, R. Guda, M. M. Haley and T. Goodson III, *J. Am. Chem. Soc.*, 2006, **128**, 13972–13973.

33 M. Long, L. Tang, D. Wang, Y. Li and Z. Shuai, *ACS Nano*, 2011, **5**, 2593–2600.

34 X. Qian, Z. Ning, Y. Li, H. Liu, C. Ouyang, Q. Chen and Y. Li, *Dalton Trans.*, 2012, **41**, 730–733.

35 B. G. Shohany, M. R. Roknabadi and A. Kompany, *Physica E*, 2016, **84**, 146–151.

36 L. Sun, P. H. Jiang, H. J. Liu, D. D. Fan, J. H. Liang, J. Wei, L. Cheng, J. Zhang and J. Shi, *Carbon*, 2015, **90**, 255–259.

37 K. Srinivasu and S. K. Ghosh, *J. Phys. Chem. C*, 2012, **116**, 5951–5956.

38 H. Zhang, X. Zhao, M. Zhang, Y. Luo, G. Li and M. Zhao, *J. Phys. D: Appl. Phys.*, 2013, **46**, 495307.

39 Y. J. Du, M. Hankel, Z. Zhu, V. Rudolph and S. C. Smith, *Chem. Commun.*, 2011, **47**, 11843–11845.

40 H. Zhang, Y. Xia, H. Bu, X. Wang, M. Zhang, Y. Luo and M. Zhao, *J. Appl. Phys.*, 2013, **113**, 044309.

41 Z. Xu, X. Lv, J. Li, J. Chen and Q. Liu, *RSC Adv.*, 2016, **6**, 25594–25600.

42 Z.-Z. Lin, *Carbon*, 2016, **108**, 343–350.

43 H. Qi, P. Yu, Y. Wang, G. Han, H. Liu, Y. Yi, Y. Li and L. Mao, *J. Am. Chem. Soc.*, 2015, **137**, 5260–5263.

44 H. Yu, A. Du, Y. Song and D. J. Searles, *J. Phys. Chem. C*, 2013, **117**, 21643–21650.

45 X. Qian, H. Liu, C. Huang, S. Chen, L. Zhang, Y. Li, J. Wang and Y. Li, *Sci. Rep.*, 2015, **5**, 7756.

46 T. Lin and J. Wang, *ACS Appl. Mater. Interfaces*, 2018, DOI: 10.1021/acsami.8b02671.

47 J. He, S. Y. Ma, P. Zhou, C. X. Zhang, C. He and L. Z. Sun, *J. Phys. Chem. C*, 2012, **116**, 26313–26321.

48 Z. Jia, Y. Li, Z. Zuo, H. Liu, C. Huang and Y. Li, *Acc. Chem. Res.*, 2017, **10**, 2470–2478.

49 Y. Xue, B. Huang, Y. Yi, Y. Guo, Z. Zuo, Y. Li, Z. Jia, H. Liu and Y. Li, *Nat. Commun.*, 2018, **9**, 1460.

50 H. Yu, Y. Xue, L. Hui, C. Zhang, Y. Li, Z. Zuo, Y. Zhao, Z. Li and Y. Li, *Adv. Mater.*, 2018, **30**, 1707082.

51 J. He, N. Wang, Z. Cui, H. Du, L. Fu, C. Huang, Z. Yang, X. Shen, Y. Yi, Z. Tu and Y. Li, *Nat. Commun.*, 2017, **8**, 1172.

52 H. Shang, Z. Zuo, L. Li, F. Wang, H. Liu, Y. Li and Y. Li, *Angew. Chem., Int. Ed.*, 2018, **57**, 774–778.

53 H. Shang, Z. Zuo, L. Yu, F. Wang, F. He and Y. Li, *Adv. Mater.*, 2018, **30**, 1801459.

54 N. N. Greenwood and A. Earnshaw, *Chemistry of the Elements*, Butterworth-Heinemann, 2nd edn, 1997.

55 A. K. Srivastava and N. Misra, *Int. J. Quantum Chem.*, 2017, **117**, 208–212.

56 E. Tahmasebi, E. Shakerzadeh and Z. Biglari, *Appl. Surf. Sci.*, 2016, **363**, 197–208.

57 A. D. Becke, *Phys. Rev. A: At., Mol., Opt. Phys.*, 1988, **38**, 3098.

58 C. Lee, W. Yang and R. G. Parr, *Phys. Rev. B: Condens. Matter Mater. Phys.*, 1988, **37**, 785–789.

59 M. J. Frisch, G. W. Trucks, H. B. Schlegel, G. E. Scuseria, M. A. Robb, J. R. Cheeseman, G. Scalmani, V. Barone, B. Mennucci, G. A. Petersson, H. Nakatsuji, M. Caricato, X. Li, H. P. Hratchian, A. F. Izmaylov, J. Bloino, G. Zheng, J. L. Sonnenberg, M. Hada, M. Ehara, K. Toyota, R. Fukuda, J. Hasegawa, M. Ishida, T. Nakajima, Y. Honda, O. Kitao, H. Nakai, T. Vreven, J. A. Montgomery, Jr., J. E. Peralta, F. Ogliaro, M. Bearpark, J. J. Heyd, E. Brothers, K. N. Kudin, V. N. Staroverov, R. Kobayashi, J. Normand, K. Raghavachari, A. Rendell, J. C. Burant, S. S. Iyengar, J. Tomasi, M. Cossi, N. Rega, J. M. Millam, M. Klene, J. E. Knox, J. B. Cross, V. Bakken, C. Adamo, J. Jaramillo, R. Gomperts, R. E. Stratmann, O. Yazyev, A. J. Austin, R. Cammi, C. Pomelli, J. W. Ochterski, R. L. Martin, K. Morokuma, V. G. Zakrzewski, G. A. Voth, P. Salvador, J. J. Dannenberg, S. Dapprich, A. D. Daniels, O. Farkas, J. B. Foresman, J. V. Ortiz, J. Cioslowski and D. J. Fox, *Gaussian 09 (Revision D. 01)*, Gaussian, Inc., Wallingford CT, 2009.

60 S. Grimme, J. Antony, S. Ehrlich and H. Krieg, *J. Chem. Phys.*, 2010, **132**, 154104.

61 S. Grimme, *J. Comput. Chem.*, 2006, **27**, 1787–1799.

62 S. Grimme, *J. Comput. Chem.*, 2004, **25**, 1463–1473.

63 J. Zhao and J. Wang, *J. Phys. Chem. C*, 2017, **121**, 21430–21438.

64 E. D. Glendening, J. K. Badenhoop, A. E. Reed, J. E. Carpenter, J. A. Bohmann, C. M. Morales, C. R. Landis and F. Weinhold, NBO 6.0., Theoretical Chemistry Institute, University of Wisconsin, Madison, WI, 2013, http://nbo6.chem.wisc.edu/.

65 T. Yanaia, D. P. Tew and N. C. Handy, *Chem. Phys. Lett.*, 2004, **393**, 51–57.

66 S.-I. Lu, *J. Comput. Chem.*, 2011, **32**, 730–736.

67 W.-M. Sun, L.-T. Fan, Y. Li, J.-Y. Liu, D. Wu and Z.-R. Li, *Inorg. Chem.*, 2014, **53**, 6170–6178.

68 X. Li, H. Ren and X. Y. J. Song, *Spectrochim. Acta, Part A*, 2015, **144**, 258–265.

69 L. Zhang, D. Qi, L. Zhao, C. Chen, Y. Bian and W. Li, *J. Phys. Chem. A*, 2012, **116**, 10249–10256.

70 X. Li, K. H. Hopmann, J. Hudecová, J. Isaksson, J. Novotná, W. Stensen, V. Andrushchenko, M. Urbanová, J.-S. Svendsen, P. Bouř and K. Ruud, *J. Phys. Chem. A*, 2013, **117**, 1721–1736.

71 N. M. O'Boyle, A. L. Tenderholt and K. M. Langner, *J. Comput. Chem.*, 2008, **29**, 839–845.

72 W. Humphrey, A. Dalke and K. Schulten, *J. Mol. Graphics*, 1996, **14**, 33–38.

73 D. R. Kanis, M. A. Ratner and T. J. Marks, *Chem. Rev.*, 1994, **94**, 195–242.
74 X. Li, H. Ren, X. Yang and J. Song, *Spectrochim. Acta, Part A*, 2015, **144**, 258–265.
75 H. D. Cohen and C. C. J. Roothaan, *J. Chem. Phys.*, 1965, **43**, S34–S39.
76 A. D. Buckhgham and B. J. Orr, *Q. Rev., Chem. Soc.*, 1967, **21**, 195–212.
77 S. Kamalinahad, M. Solimannejad and E. Shakerzadeh, *Bull. Chem. Soc. Jpn.*, 2016, **89**, 692–699.
78 F. Ma, Z.-J. Zhou and Y.-T. Liu, *ChemPhysChem*, 2012, **13**, 1307–1312.
79 A. K. Srivastava and N. Misra, *J. Mol. Model.*, 2015, **21**, 305.
80 Y. Y. Melcamu, S. Wen, L. Yan, T. Zhang and Z. Su, *Mol. Simul.*, 2013, **39**, 214–219.
81 A. K. Srivastava and N. Misra, *Int. J. Quantum Chem.*, 2017, **117**, 208–212.
82 X. Li, S. Li, H. Ren, J. Yang and Y. Tang, *Nanomaterials*, 2017, **7**, 184.
83 J. L. Oudar, *J. Chem. Phys.*, 1977, **67**, 446.